

# Roll-to-Roll Encapsulation of Metal Nanowires between Graphene and Plastic Substrate for High-Performance Flexible Transparent Electrodes

Bing Deng,<sup>†</sup> Po-Chun Hsu,<sup>‡</sup> Guanchu Chen,<sup>†</sup> B. N. Chandrashekar,<sup>†</sup> Lei Liao,<sup>†</sup> Zhawulie Ayitimuda,<sup>§</sup> Jinxiong Wu,<sup>†</sup> Yunfan Guo,<sup>†</sup> Li Lin,<sup>†</sup> Yu Zhou,<sup>†</sup> Mahaya Aisijiang,<sup>§</sup> Qin Xie,<sup>†</sup> Yi Cui,<sup>\*,‡,||</sup> Zhongfan Liu,<sup>\*,†</sup> and Hailin Peng<sup>\*,†</sup>

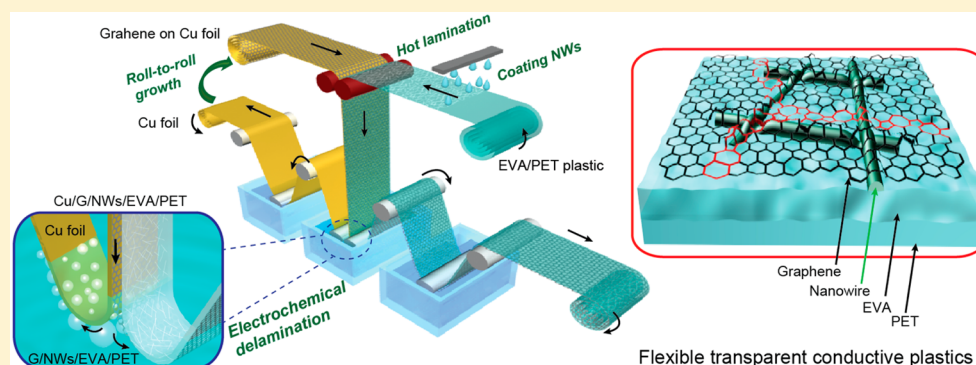
<sup>†</sup>Center for Nanochemistry, Beijing Science and Engineering Center for Nanocarbons, Beijing National Laboratory for Molecular Sciences (BNLMS), College of Chemistry and Molecular Engineering, Peking University, Beijing 100871, People's Republic of China

<sup>‡</sup>Department of Materials Science and Engineering, Stanford University, Stanford, California 94305, United States

<sup>§</sup>College of Chemistry and Biological Sciences, Yili Normal University, Yining, Xinjiang 83500, People's Republic of China

<sup>||</sup>Stanford Institute for Materials and Energy Sciences, SLAC National Accelerator Laboratory, 2575 Sand Hill Road, Menlo Park, California 94025, United States

## S Supporting Information



**ABSTRACT:** Transparent conductive film on plastic substrate is a critical component in low-cost, flexible, and lightweight optoelectronics. Industrial-scale manufacturing of high-performance transparent conductive flexible plastic is needed to enable wide-ranging applications. Here, we demonstrate a continuous roll-to-roll (R2R) production of transparent conductive flexible plastic based on a metal nanowire network fully encapsulated between graphene monolayer and plastic substrate. Large-area graphene film grown on Cu foil via a R2R chemical vapor deposition process was hot-laminated onto nanowires precoated EVA/PET film, followed by a R2R electrochemical delamination that preserves the Cu foil for reuse. The encapsulated structure minimized the resistance of both wire-to-wire junctions and graphene grain boundaries and strengthened the adhesion of nanowires and graphene to plastic substrate, resulting in superior optoelectronic properties (sheet resistance of  $\sim 8 \Omega \text{ sq}^{-1}$  at 94% transmittance), remarkable corrosion resistance, and excellent mechanical flexibility. With these advantages, long-cycle life flexible electrochromic devices are demonstrated, showing up to 10000 cycles.

**KEYWORDS:** Flexible transparent electrode, metal nanowires, graphene, roll-to-roll, encapsulation

Transparent conductive electrodes are important components for various optoelectronic devices such as thin-film solar cell, organic light emitting diodes (OLED), touch screens, and smart windows.<sup>1–4</sup> The use of indium tin oxide (ITO) as a conventional transparent electrode material hinders the application in flexible electronics due to film brittleness, low infrared transmittance, scarcity of indium, and high-cost of the preparation procedure.<sup>5,6</sup> To overcome the deficiencies of ITO, many alternative nanomaterials have been studied including metal nanowires (NWs),<sup>7–13</sup> carbon nanotubes (CNTs),<sup>14–16</sup> and graphene.<sup>3,17,18</sup> As for metal NWs, post-treatment is

essential to deal with the high wire-to-wire junction resistance,<sup>7,8,19</sup> the low corrosion resistance,<sup>20,21</sup> the surface roughness,<sup>22</sup> and the low adherence to the substrate.<sup>21,23</sup> Efforts have been made to fabricate hybrid electrodes of graphene and metal NWs to enhance the overall performance.<sup>24–29</sup> As flexible building blocks, metal NWs provide highly conducting pathways that connect graphene domains, while graphene

**Received:** April 21, 2015

**Revised:** May 19, 2015

**Published:** May 28, 2015

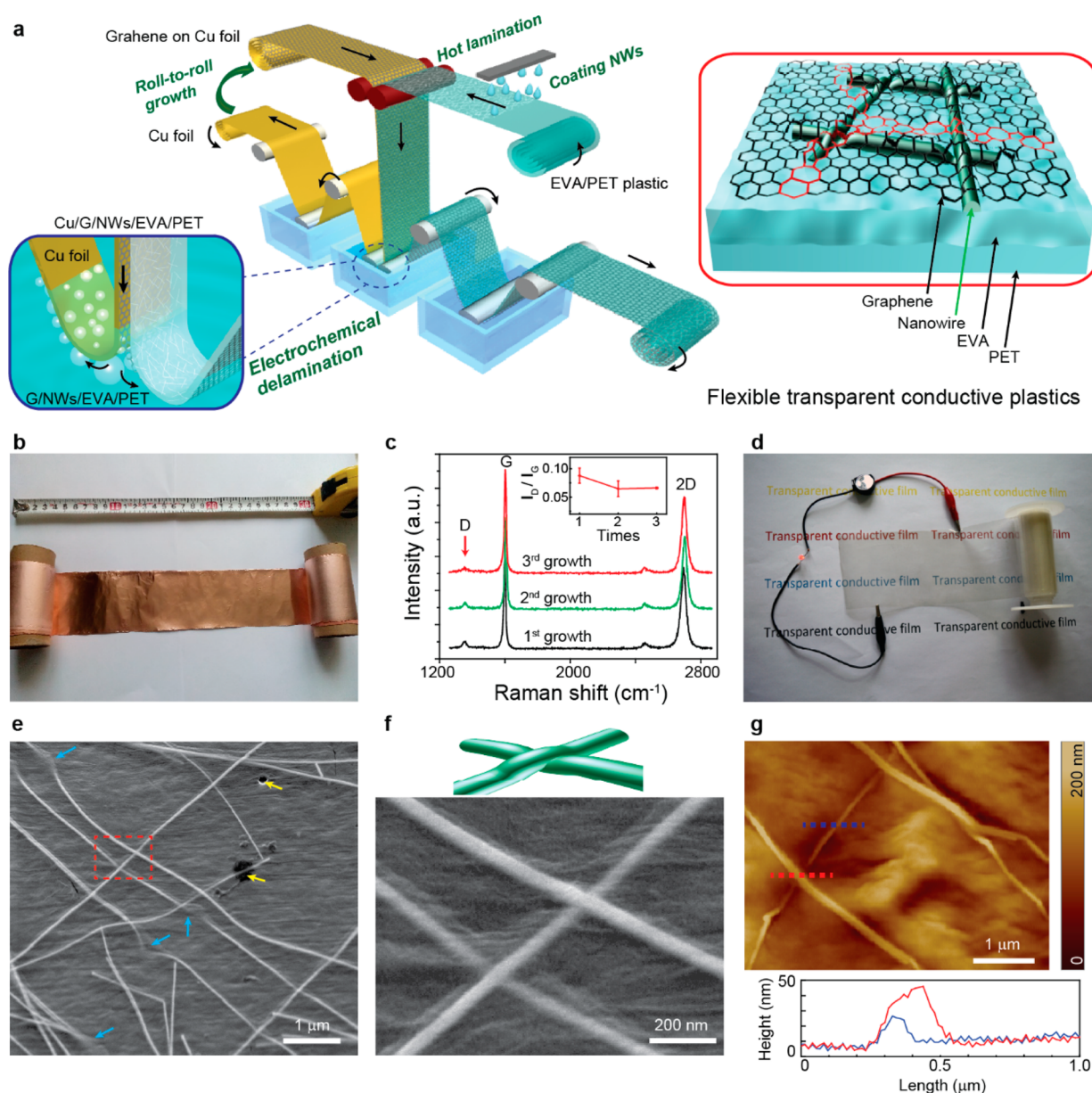


**Figure 1.** Schematic and structure of graphene and metal nanowire hybrid films produced by a continuous roll-to-roll process. (a) Schematic diagram of the fabrication process includes coating of metal nanowires on polymer substrate (EVA/PET), hot-press lamination with graphene/Cu foil, delamination of graphene and Cu foil by electrochemical bubbling method, and the reuse of Cu foil to grow graphene by a continuous chemical vapor deposition system. The detailed structural schematic of the hybrid film labeled in the red cycle shows that nanowires are partly embedded into the EVA substrate and fully encapsulated by monolayer graphene film. (b) A photograph of a roll of graphene/Cu foil with length of 5 m and width of 5 cm grown by roll-to-roll chemical vapor deposition. (c) Raman spectra of graphene films transferred onto SiO<sub>2</sub>/Si. Inset shows the  $I_D/I_G$  (D to G peak intensity ratio) varies with the times of growth, revealing the improved quality of graphene. (d) A photograph of a roll of hybrid film of graphene and AgNWs on EVA/PET plastic with length of 5 m and width of 5 cm, which can lighten up a red LED indicator. (e) SEM image of the hybrid film of graphene and AgNWs on the EVA/PET plastic, showing that AgNWs are partly embedded into EVA substrate and fully covered by monolayer graphene. The fully embedded portions of AgNWs are indicated by blue arrows. The pinholes of graphene are indicated by yellow arrows. (f) Enlarged side-view SEM image of the hybrid film of graphene and AgNWs, showing a good contact of AgNW junctions. (g) AFM image of the hybrid film of graphene and AgNWs, showing that AgNWs are partly embedded into the polymer substrate.

may protect metal NWs from oxidation and corrosion. In this regard, the quality and coverage area of graphene layers determine how effective this passivation layer is. Nevertheless, combining metal NWs and graphene in an efficient procedure to realize all the post-treatment with industrial-scale fabrication remains a challenge.

Here we developed a full roll-to-roll (R2R) production of high-performance flexible transparent electrodes based on metal NWs fully encapsulated by a large-area monolayer

graphene film and a flexible transparent plastic substrate. In our proposed method, there are four essential steps to realize the R2R encapsulation procedure (Figure 1a): (i) R2R growth of a large-area monolayer graphene film on an industrial Cu foil via chemical vapor deposition (CVD); (ii) coating or transfer of metal nanowires onto the commercial ethylene vinyl acetate/polyethylene terephthalate (EVA/PET) plastic film; (iii) hot-lamination of graphene/Cu foil onto metal NWs precoated EVA/PET plastic; and (iv) electrochemical bubbling delami-

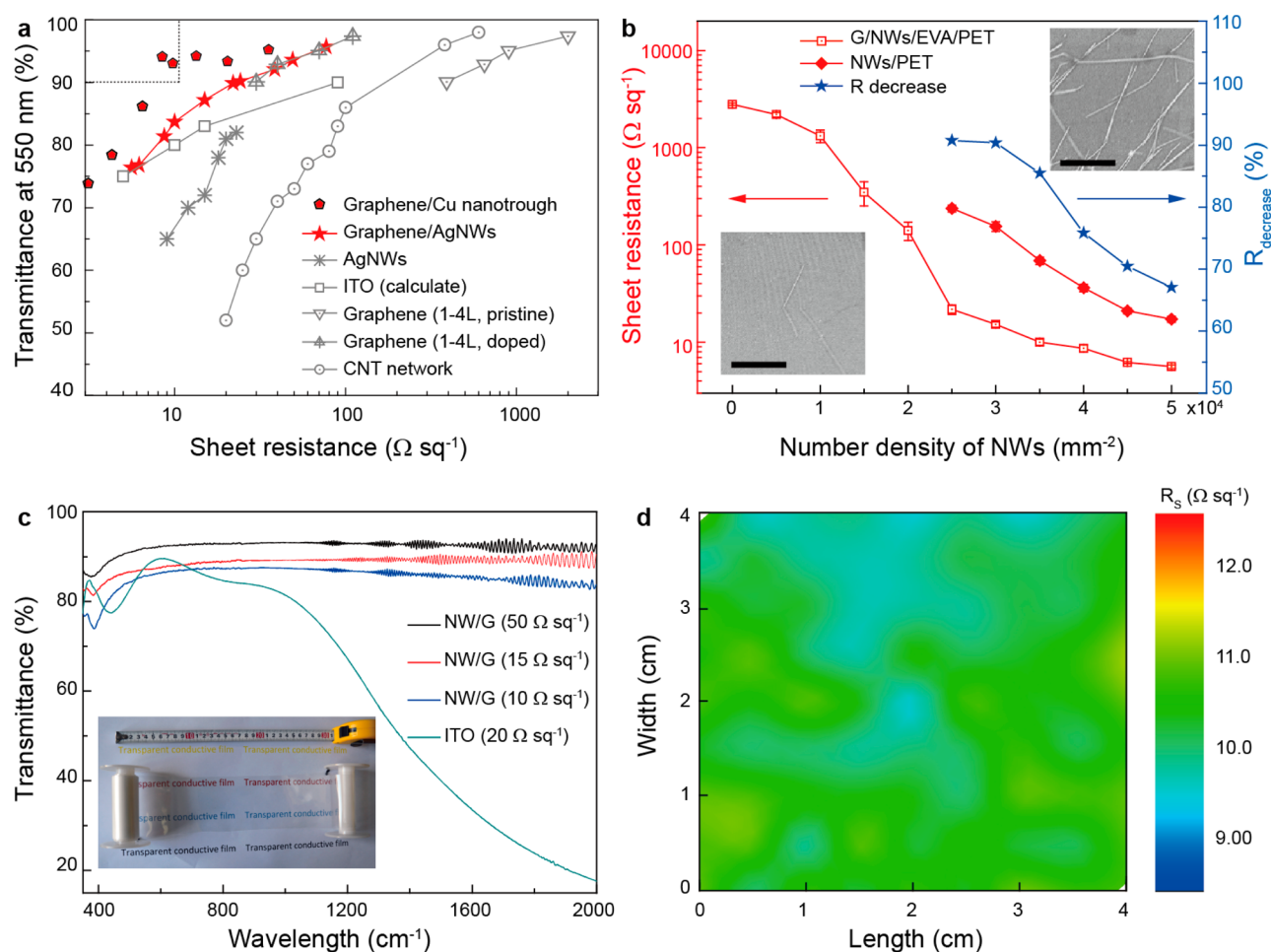


**Figure 2.** Graphene and metal nanowire hybrid films as transparent, conductive electrodes. (a) Sheet resistance versus optical transmission (at 550 nm) for the hybrid film of graphene and AgNWs or Cu nanotrough. The performances of AgNWs,<sup>8</sup> ITO,<sup>3</sup> pristine graphene,<sup>3</sup>  $\text{HNO}_3$ -doped graphene,<sup>3</sup> and CNTs<sup>16</sup> are shown for comparison. Note that the measured transmittance mentioned does not include the absorption and reflectance from the substrate. (b) Sheet resistance versus number density of AgNWs for pure AgNW film and graphene/AgNW hybrid film. (Inset) SEM image of hybrid films with different nanowire densities, scale bar:  $1 \mu\text{m}$ . (c) UV-vis-NIR spectra of graphene/AgNW hybrid films with different sheet resistance, showing a flat spectrum for broad wavelength range and much better near-infrared transmittance than a commercial ITO electrode. (d) A 2D mapping image of the sheet resistance for a graphene/AgNW hybrid film with the size of  $4 \times 4 \text{ cm}^2$ , showing considerable uniformity of conductivity.

nation of graphene film from Cu foil. Detailed Experimental Section can be seen in Supporting Information.

First, we grow a roll of continuous graphene film on an industrial Cu foil with size of 5 cm in width and 5 m in length using continuous R2R low-pressure CVD method (Figure 1b). Supporting Information Movie S1 shows the roll-to-roll growth of graphene. Note that the graphene grown by this R2R process is almost monolayer continuous film which has high optical transmittance and electrical conductivity (Supporting Information Figure S2). Remarkably, the Cu foil can be preserved after the subsequent process of electrochemical transfer and reused for graphene growth. Three cycles of growth of graphene were conducted, and their quality was compared using Raman spectroscopy. Figure 1c shows the evolution of Raman spectra for a series of monolayer graphene films repeatedly grown and transferred from the same Cu foil. As the growth cycle increases, the characteristic disorder-induced D band at  $\sim 1350 \text{ cm}^{-1}$  decreases. This observation indicated that the quality of graphene R2R grown on the reused Cu foil was enhanced, which presumably was attributed to the surface flattening and grain size enlargement of Cu foil during repeated high-

temperature annealing and graphene growth (Supporting Information Figure S3).

Second, metal nanowires were coated on an EVA/PET ( $50 \mu\text{m}/75 \mu\text{m}$  thick) sheet using a Mayer rod,<sup>8</sup> where EVA is mostly used as high-quality adhesive transparent films for encapsulating commercial solar panels and PET is a typical flexible transparent plastic substrate. The EVA surface is pretreated by air plasma (power for 99 W, time for 2 min) to enhance its hydrophilicity because of the formation of polar oxygen groups,<sup>29</sup> which is beneficial for the uniform dispersion of NW suspension on the EVA/PET substrate (Supporting Information Figure S4). In this work, silver NWs (AgNWs) and copper NWs (CuNWs) were tested. The AgNWs or CuNWs form a conductive network whose number density can be controlled by the coating conditions such as concentration of NW suspension. In addition, CuNW networks consisting of copper nanotrough (CuNT)<sup>12</sup> with different mesh densities were transferred onto the EVA/PET film.

Then the graphene film grown on Cu foil was hot-laminated onto the NWs/EVA/PET film to form Cu/graphene/NWs/EVA/PET laminated structure at the temperature of  $\sim 100^\circ\text{C}$



by two rollers providing heat and mechanical pressure simultaneously<sup>30,31</sup> (Supporting Information Movie S2). The EVA layer melts at the specific temperature to partially embed NWs on its surface and adhere to the graphene/Cu film. This process ensures good contact of graphene and NWs with minimal formation of air traps, cracks and wrinkles of graphene, forming a Cu/graphene/NWs/EVA/PET laminated structure.

Finally, the graphene film is continuously R2R delaminated from Cu foil by an efficient electrochemical bubbling delamination transfer method<sup>32,33</sup> (Supporting Information Figure S5 and Movie S3). Note that the Cu/graphene/NWs/EVA/PET cathode was partially immersed in water (Supporting Information Figure S5b), where a large amount of hydrogen bubbles can generate and propagate in the confined area through water electrolysis, thus efficiently delaminate the graphene film and Cu foil at very low electrolysis voltage. The transfer speed is much faster than previously reported works<sup>32,33</sup> based on electrochemical delamination method and can reach up to 2 cm/s, which is enough for an efficient roll-to-roll process. Because the cathode is negatively charged during delamination process, the obtained graphene/NWs/EVA/PET films can avoid oxidation while the Cu foil can be preserved for further R2R CVD growth of graphene.

Figure 1d shows a typical photograph of a roll of graphene/AgNWs/EVA/PET plastic with the size of 5 m long and 5 cm wide, which can act as a flexible transparent tape to light up a red LED indicator (3.0 V, 20 mA). The microstructure of the encapsulated graphene/NWs/plastic film was characterized by scanning electron microscopy (SEM) and atomic force microscopy (AFM). Pure AgNWs coated on a PET substrate were first characterized by AFM, in which case the junction of two NWs is weakly connected. From the profile of AFM (Supporting Information Figure S7), the diameter of an individual AgNW is about 35 nm and a junction of two AgNWs is about 70 nm, which implies that the two adjacent NWs are simply stacked rather than fused together. As for the encapsulated graphene/AgNWs/EVA/PET film, the AgNWs are covered by a continuous graphene monolayer without creating cracks of graphene (Figure 1e), which is significant for the role of graphene as a protective layer against corrosion for AgNWs. The AgNWs are partially embedded into the EVA layer according to the decrease in height of single NW from ~35 nm to ~15 nm (Figure 1g, blue line). This embedding behavior reduces the surface roughness and also benefits the passivation of AgNWs by decreasing the exposure area of AgNWs to the environment.<sup>21</sup>

It has been reported that heat annealing and mechanical pressure contribute to the fusing of junctions of silver nanowires.<sup>7,34</sup> The hot-lamination process provides simultaneously heat and mechanical pressure and causes the fusing of junctions according to the side-view SEM image (Figure 1f). The junction fusion can also be demonstrated in AFM by the reduced height of junctions from 70 nm (Supporting Information Figure S7b, red line) to ~40 nm (Figure 1g, red line). The flattening and fusion of NW junctions enable excellent optical and electrical properties of NW network electrodes. The bridge effect of AgNWs and graphene domains also facilitates the electrical conduction of the hybrid film. As shown in Figure 2a, encapsulated graphene/CuNT/EVA/PET hybrid films exhibit excellent optoelectronic properties (94% optical transmittance at 550 nm with sheet resistance of ~8  $\Omega$  sq<sup>-1</sup>). The encapsulated graphene/AgNWs/EVA/PET films also show outstanding performance with 90% optical trans-

mittance (550 nm) at 22  $\Omega$  sq<sup>-1</sup> and 84% at 10  $\Omega$  sq<sup>-1</sup>, superior to other transparent electrodes based on solution-processed AgNWs or CuNWs, ITO, pristine CVD graphene, chemical-doped CVD graphene, and carbon nanotubes.<sup>3,5,7,8,10,16,35</sup>

The sheet resistance of the encapsulated graphene/NWs/EVA/PET films can be tuned by varying the number density of NWs (Figure 2b). For pure AgNW film whose number density is larger than a percolation critical density,  $N_c$ , continuous NW network can be formed, and electrons can percolate across this NW network.<sup>36</sup> Hence, if the number density of AgNWs is larger than  $N_c$ , the conductance is dominated by the relatively high conductive AgNW networks, rather than graphene (Figure 2b). Note that in this number density region, the encapsulated AgNW film shows 60–90% decrease in sheet resistance than the random pure AgNWs networks with the same NW number densities, which is presumably due to the graphene conduction channel and the decrease of the internanowire contact resistance due to the fusion of wire-to-wire junction in the hot-lamination process as discussed above. When the number density of AgNWs is smaller than  $N_c$  (Figure 2b), the conductivity of encapsulated AgNW film is mostly dominated by the graphene channel. Moreover, the encapsulated film possesses lower resistance than pristine graphene because the AgNWs act as additional conduction channels across graphene grain boundaries to bridge graphene domains.<sup>25,37</sup>

In addition to the outstanding electrical property, the encapsulated graphene/AgNWs/EVA/PET film demonstrates a flat, high transmittance in a broad wide spectrum from 400 to 2000 nm, much better than the commercial ITO electrode that is opaque in the near-infrared region (Figure 2c). Wideband flat spectra of the transparent electrode is beneficial for many optoelectronic devices such as near-infrared sensors and may improve the efficiency of solar cell by using light energy in the near-infrared region.<sup>38,39</sup> For practical applications where production yield and controllability are critical, high uniformity in the conductivity of transparent electrode is essential. As shown in Figure 2d, a sheet resistance distribution of an encapsulated graphene/AgNWs/EVA/PET film with the area of 4 × 4 cm<sup>2</sup> tested at the interval of 0.5 × 0.5 cm<sup>2</sup> reveals a mean value of 10.3  $\Omega$  sq<sup>-1</sup> and a standard deviation of 0.4  $\Omega$  sq<sup>-1</sup>, which indicates a reasonably high electrical homogeneity. The homogeneity of conductivity is attributed to the optimized coating conditions of NWs and the usage of graphene. The AgNWs film coated on substrate is a conductive mesh with many holes. This porous structure results in inhomogeneity because of the nonconductive and open spaces within the networks. On the contrast, for the graphene encapsulated AgNWs electrode, graphene occupies empty spaces in the nanowire networks, allowing the charge transport across the original nonconductive open space, which greatly improves the electrical homogeneity.<sup>40</sup>

Corrosion resistance is a significant concern for metal NWs-based transparent electrodes because the chemical instability and the ease of oxidation may hinder the practical applications of AgNW and CuNW electrodes. Surface passivation of AgNW and CuNW films is necessary to significantly improve their chemical stability. It has been reported that graphene is chemically inert<sup>41</sup> and can be used for corrosion-inhibiting coating for metallic nanostructures<sup>27</sup> that are susceptible to atmospheric corrosion.<sup>42</sup> Metal NW network films can be hybridized with the reduced graphene oxide (RGO) nanosheets for the improvement of stability.<sup>27</sup> However, it is difficult to fulfill a uniform large-area lamination using the RGO



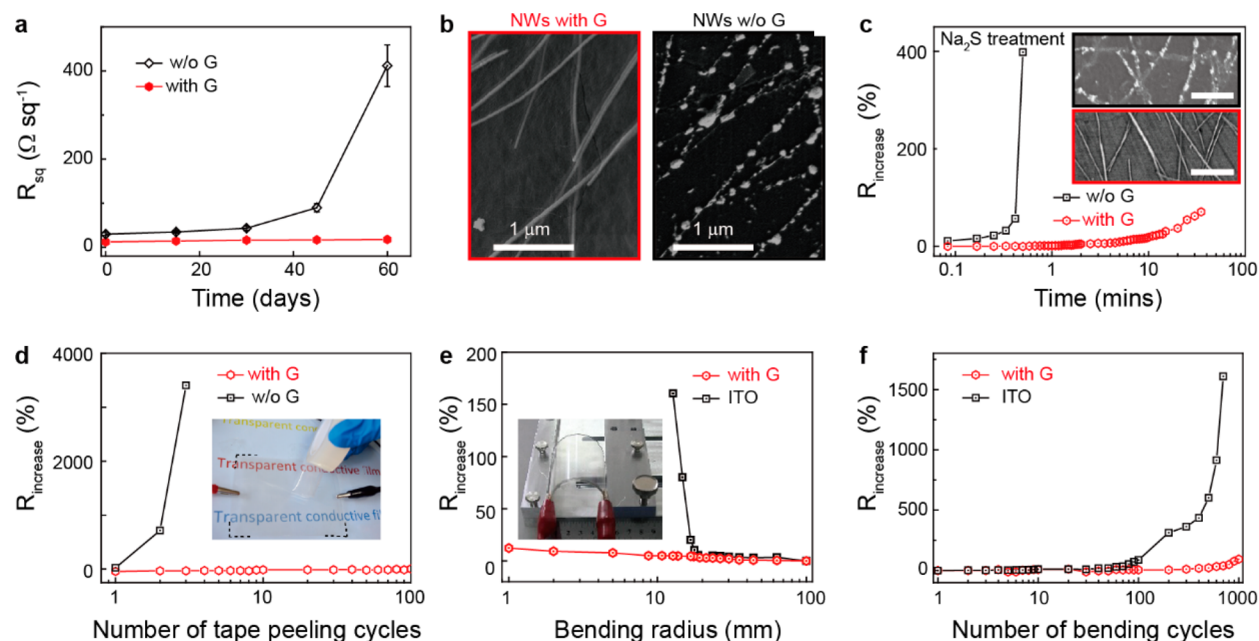


**Figure 3.** The durability of graphene and metal nanowire hybrid transparent electrodes. (a) Changes in sheet resistance of pure AgNW films and the graphene/AgNW hybrid films exposed in air at room temperature for 2 months. (b) SEM image of the graphene/AgNW hybrid film and pure AgNW films exposed in air for 2 months, revealing that AgNWs without the protection of graphene were oxidized to break. (c) Changes in sheet resistance of pure AgNW films and the graphene/AgNW hybrid films under the attack of aqueous  $\text{Na}_2\text{S}$  (4 wt %). (Inset) Morphologies of AgNWs with or without the graphene coverage attacked for 30 s, respectively. Scale bar: 1  $\mu\text{m}$ . (d) Variations in sheet resistance of pure AgNW films and graphene/AgNW hybrid films as a function of the number of cycles of repeated peeling by 3M Scotch tape. (e) Variations in sheet resistance versus bending radius for the hybrid transparent plastic electrodes and ITO films on 150  $\mu\text{m}$  thick PET. (f) Variations in sheet resistance of the hybrid transparent plastic electrodes and ITO films on PET as a function of the number of cycles of repeated bending to a radius of 20 mm.

nanosheets. In contrast, our fully encapsulated graphene/AgNWs/EVA/PET films demonstrate outstanding chemical stability and corrosion resistance. Figure 3a shows the changes in resistances in an uncovered AgNWs/EVA/PET film and an encapsulated graphene/AgNWs/EVA/PET film with the same number density of AgNWs upon exposure in atmosphere at room temperature for two months. The graphene encapsulated AgNW films show long-term chemical stability, superior to the uncoated AgNW films. The morphology of the encapsulated film remained unchanged while the exposed AgNWs were corroded after exposure in air for two months (Figure 3b). On the other hand, copper is more susceptible to corrosion than silver. The encapsulated graphene/CuNT/EVA/PET (Supporting Information Figure S8) and graphene/CuNWs/EVA/PET (Supporting Information Figure S9) both show much better corrosion resistance than their uncovered Cu nanostructure counterparts. Remarkably, the fully encapsulated graphene/AgNWs/EVA/PET can bear chemical attack by corrosive liquids, such as sulfurization in  $\text{Na}_2\text{S}$  solution (Figure 3c). The excellent corrosion resistance of graphene/NWs/EVA/PET film can be attributed to the partially embedded structure of NWs into the EVA substrate and the full encapsulation of the inert graphene film as a passivation layer.

Another important issue of the metal NWs network-based transparent electrodes is the weak adhesion of NWs to the substrate. Usually, precoated metal NWs do not stick to and can be easily wiped off from the substrate due to the weak adhesive forces. In contrast, since the metal NWs are partially embedded into EVA substrate during the lamination process, the encapsulation of NWs between graphene and EVA layer dramatically enhanced the adhesion to the substrate. As shown in Figure 3d, the conductivity of the encapsulated graphene/

AgNWs/EVA/PET electrodes does not degrade upon repeated Scotch tape peeling test up to 100 cycles. Note that graphene film is also not damaged even after repeated peeling (Supporting Information Figure S10) because the whole graphene film adheres firmly to the EVA supporting layer. These observations indicated the full encapsulated graphene/AgNWs/EVA/PET film can withstand repeated tape peeling, far superior to the uncoated NW film electrode.

We then examined the mechanical durability of the encapsulated graphene/AgNWs/EVA/PET film by measuring the sheet resistance change at various bending tests with different radius from 100 to 1 mm (Figure 3e). In contrast to commercial ITO films on 150  $\mu\text{m}$  thick PET substrate, which easily degrade with a bending radius of less than  $\sim 20$  mm, the encapsulated films remain highly conductive with little variation in resistance up to a bending radius of 1 mm, which is comparable to the best results for both graphene films and AgNWs electrodes. In addition, unlike ITO/PET films, the encapsulated film can keep their structural integrity and mechanical stability after repeated dynamic bending tests (Figure 3f). The encapsulated film can be bent at 20 mm for 1000 bending cycles without the degradation of conductance, indicating its excellent mechanical durability. The high flexibility of the encapsulated film is essential in some flexible electronics application.

Because of many unique advantages and features of encapsulated graphene/AgNWs/EVA/PET plastic electrodes, including facile large-scale R2R manufacturing, high broadband transparency, super electrical conductivity, remarkable corrosion resistance, strong adhesion to substrates, excellent flexibility, and outstanding mechanical durability, these electrodes are readily applicable to the fabrication of practical



In conclusion, fully encapsulated graphene/nanowire/plastic films are fabricated by a continuous large-scale roll-to-roll production for transparent conductive electrodes, which shows high optoelectronic performance, remarkable corrosion resistance, good flexibility, and strong adhesion to substrate. This method can be easily extended to build other graphene-encapsulated nanostructures such as 2D colloid crystals, carbon nanotubes, and nanoparticles. The high-efficiency roll-to-roll procedure shows its potential in mass production of various encapsulated nanostructures in low cost, which may accelerate its application in industry.

## ■ ASSOCIATED CONTENT

### Supporting Information

Experimental details, supplementary figures and videos. The Supporting Information is available free of charge on the ACS Publications website at DOI: 10.1021/acs.nanolett.5b01531.

## ■ AUTHOR INFORMATION

### Corresponding Authors

\*E-mail: hlpeng@pku.edu.cn.

\*E-mail: yicui@stanford.edu.

\*E-mail: zfliu@pku.edu.cn.

### Author Contributions

B.D. and P.-C.H. contributed equally to this work.

H.P., B.D., and P.H. conceived and designed the experiments. B.D. and P.H. performed the synthesis, structural characterization, device fabrication, measurements, and analyses. G.C., B.N.C., L.L., Z.A., J.W., Y.G., L.L., Y.Z., M.A., and Q. X. assisted in experimental work and contributed to the scientific discussions. B.D., P.H., and H.P. wrote the paper. H.P., Y.C., and Z.L. supervised the project. All the authors discussed the results and commented on the manuscript.

### Notes

The authors declare no competing financial interest.

## ■ ACKNOWLEDGMENTS

This work was financially supported by the National Basic Research Program of China (Nos. 2014CB932500, 2011CB921904, and 2013CB932603), the National Natural Science Foundation of China (Nos. 21173004, 21222303, 51121091, and 51362029), National Program for Support of Top-Notch Young Professionals, and Beijing Municipal Science & Technology Commission (No. Z131100003213016).

## ■ REFERENCES

- (1) Fortunato, E.; Ginley, D.; Hosono, H.; Paine, D. C. Transparent conducting oxides for photovoltaics. *Mater. Res. Soc. Bull.* **2007**, *32*, 242–247.
- (2) Pang, S. P.; Hernandez, Y.; Feng, X. L.; Mullen, K. Graphene as Transparent Electrode Material for Organic Electronics. *Adv. Mater.* **2011**, *23*, 2779–2795.
- (3) Bae, S.; et al. Roll-to-roll production of 30-in. graphene films for transparent electrodes. *Nat. Nanotechnol.* **2010**, *5*, 574–578.
- (4) Granqvist, C. G.; et al. Recent advances in electrochromics for smart windows applications. *Sol. Energy* **1998**, *63*, 199–216.
- (5) Ellmer, K. Past achievements and future challenges in the development of optically transparent electrodes. *Nat. Photonics* **2012**, *6*, 808–816.
- (6) Kumar, A.; Zhou, C. W. The Race To Replace Tin-Doped Indium Oxide: Which Material Will Win? *ACS Nano* **2010**, *4*, 11–14.
- (7) Lee, J. Y.; Connor, S. T.; Cui, Y.; Peumans, P. Solution-Processed Metal Nanowire Mesh Transparent Electrodes. *Nano Lett.* **2008**, *8*, 689–692.
- (8) Hu, L. B.; Kim, H. S.; Lee, J. Y.; Peumans, P.; Cui, Y. Scalable Coating and Properties of Transparent, Flexible, Silver Nanowire Electrodes. *ACS Nano* **2010**, *4*, 2955–2963.
- (9) Scardaci, V.; Coull, R.; Lyons, P. E.; Rickard, D.; Coleman, J. N. Spray Deposition of Highly Transparent, Low-Resistance Networks of Silver Nanowires over Large Areas. *Small* **2011**, *7*, 2621–2628.
- (10) Rathmell, A. R.; Wiley, B. J. The Synthesis and Coating of Long, Thin Copper Nanowires to Make Flexible, Transparent Conducting Films on Plastic Substrates. *Adv. Mater.* **2011**, *23*, 4798–4803.
- (11) Zhang, D. Q.; et al. Synthesis of Ultralong Copper Nanowires for High-Performance Transparent Electrodes. *J. Am. Chem. Soc.* **2012**, *134*, 14283–14286.
- (12) Wu, H.; et al. A transparent electrode based on a metal nanotrough network. *Nat. Nanotechnol.* **2013**, *8*, 421–425.
- (13) Hsu, P. C.; et al. Electrolessly Deposited Electrospun Metal Nanowire Transparent Electrodes. *J. Am. Chem. Soc.* **2014**, *136*, 10593–10596.
- (14) Wu, Z. C.; et al. Transparent, conductive carbon nanotube films. *Science* **2004**, *305*, 1273–1276.
- (15) Zhang, M.; et al. Strong, transparent, multifunctional, carbon nanotube sheets. *Science* **2005**, *309*, 1215–1219.
- (16) Geng, H. Z.; et al. Effect of Acid Treatment on Carbon Nanotube-Based Flexible Transparent Conducting Films. *J. Am. Chem. Soc.* **2007**, *129*, 7758–7759.
- (17) Bonaccorso, F.; Sun, Z.; Hasan, T.; Ferrari, A. C. Graphene photonics and optoelectronics. *Nat. Photonics* **2010**, *4*, 611–622.
- (18) Kim, K. S.; et al. Large-scale pattern growth of graphene films for stretchable transparent electrodes. *Nature* **2009**, *457*, 706–710.
- (19) Garnett, E. C.; et al. Self-limited plasmonic welding of silver nanowire junctions. *Nat. Mater.* **2012**, *11*, 241–249.
- (20) Hsu, P. C.; et al. Passivation Coating on Electrospun Copper Nanofibers for Stable Transparent Electrodes. *ACS Nano* **2012**, *6*, 5150–5156.
- (21) Zeng, X. Y.; Zhang, Q. K.; Yu, R. M.; Lu, C. Z. A New Transparent Conductor: Silver Nanowire Film Buried at the Surface of a Transparent Polymer. *Adv. Mater.* **2010**, *22*, 4484–4488.
- (22) Yu, Z. B.; et al. Highly Flexible Silver Nanowire Electrodes for Shape-Memory Polymer Light-Emitting Diodes. *Adv. Mater.* **2011**, *23*, 664–668.
- (23) Akter, T.; Kim, W. S. Reversibly Stretchable Transparent Conductive Coatings of Spray-Deposited Silver Nanowires. *ACS Appl. Mater. Interfaces* **2012**, *4*, 1855–1859.
- (24) Kholmanov, I. N.; et al. Improved Electrical Conductivity of Graphene Films Integrated with Metal Nanowires. *Nano Lett.* **2012**, *12*, 5679–5683.
- (25) Choi, H. O.; Kim, D. W.; Kim, S. J.; Yang, S. B.; Jung, H. T. Role of 1D Metallic Nanowires in Polydomain Graphene for Highly Transparent Conducting Films. *Adv. Mater.* **2014**, *26*, 4575–4581.
- (26) Chen, R. Y.; et al. Co-Percolating Graphene-Wrapped Silver Nanowire Network for High Performance, Highly Stable, Transparent Conducting Electrodes. *Adv. Funct. Mater.* **2013**, *23*, 5150–5158.
- (27) Kholmanov, I. N.; et al. Reduced Graphene Oxide/Copper Nanowire Hybrid Films as High-Performance Transparent Electrodes. *ACS Nano* **2013**, *7*, 1811–1816.
- (28) Chen, T. L.; Ghosh, D. S.; Mkhitarian, V.; Pruneri, V. Hybrid Transparent Conductive Film on Flexible Glass Formed by Hot-Pressing Graphene on a Silver Nanowire Mesh. *ACS Appl. Mater. Interfaces* **2013**, *5*, 11756–11761.
- (29) Moon, I. K.; et al. 2D Graphene Oxide Nanosheets as an Adhesive Over-Coating Layer for Flexible Transparent Conductive Electrodes. *Sci. Rep.* **2013**, *3*, 1112.
- (30) Martins, L. G. P.; et al. Direct Transfer of Graphene onto Flexible Substrates. *Proc. Natl. Acad. Sci. U.S.A.* **2013**, *110*, 17762–17767.
- (31) Han, G. H.; et al. Poly(Ethylene Co-Vinyl Acetate)-Assisted One-Step Transfer of Ultra-Large Graphene. *Nano* **2011**, *6*, 59–65.
- (32) Wang, Y.; et al. Electrochemical Delamination of CVD-Grown Graphene Film: Toward the Recyclable Use of Copper Catalyst. *ACS Nano* **2011**, *5*, 9927–9933.



- (33) Gao, L. B.; et al. Repeated growth and bubbling transfer of graphene with millimetre-size single-crystal grains using platinum. *Nat. Commun.* **2012**, *3*, 699–705.
- (34) Tokuno, T.; et al. Fabrication of silver nanowire transparent electrodes at room temperature. *Nano Res.* **2011**, *4*, 1215–1222.
- (35) Li, X. S.; et al. Transfer of Large-Area Graphene Films for High-Performance Transparent Conductive Electrodes. *Nano Lett.* **2009**, *9*, 4359–4363.
- (36) Ye, S.; Rathmell, A. R.; Chen, Z.; Stewart, I. E.; Wiley, B. J. Metal nanowire networks: the next generation of transparent conductors. *Adv. Mater.* **2014**, *26*, 6670–6687.
- (37) Jeong, C. W.; Nair, P.; Khan, M.; Lundstrom, M.; Alam, M. A. Prospects for Nanowire-Doped Polycrystalline Graphene Films for Ultratransparent, Highly Conductive Electrodes. *Nano Lett.* **2011**, *11*, 5020–5025.
- (38) Peng, H. L.; et al. Topological insulator nanostructures for near-infrared transparent flexible electrodes. *Nat. Chem.* **2012**, *4*, 281–286.
- (39) Guo, Y. F.; et al. Selective-Area Van der Waals Epitaxy of Topological Insulator Grid Nanostructures for Broadband Transparent Flexible Electrodes. *Adv. Mater.* **2013**, *25*, 5959–5964.
- (40) An, B. W.; et al. Stretchable and Transparent Electrodes using Hybrid Structures of Graphene-Metal Nanotrough Networks with High Performances and Ultimate Uniformity. *Nano Lett.* **2014**, *14*, 6322–6328.
- (41) Novoselov, K. S.; et al. A roadmap for graphene. *Nature* **2012**, *490*, 192–200.
- (42) Elechiguerra, J. L.; et al. Corrosion at the nanoscale: The case of silver nanowires and nanoparticles. *Chem. Mater.* **2005**, *17*, 6042–6052.
- (43) Mortimer, R. J. Electrochromic Materials. *Annu. Rev. Mater. Res.* **2011**, *41*, 241–268.